Full paper/Mémoire

The effect of framework functionality on the catalytic activation of supported Pd nanoparticles in the Mizoroki–Heck coupling reaction

Fatemeh Ashouri [a, *], Maryam Zare [b], Mojtaba Bagherzadeh [c]

[a] Department of Applied Chemistry, Faculty of Pharmaceutical Chemistry, Pharmaceutical Sciences Branch, Islamic Azad University, Tehran, Iran
[b] Department of Basic Sciences, Golpaygan University of Technology, P.O.Box 87717-65651, Golpaygan, Iran
[c] Department of Chemistry, Sharif University of Technology, P.O. Box 11155-3516, Tehran, Iran

ARTICLE INFO

ABSTRACT

Palladium nanoparticles (Pd-NPs) were supported on functional and nonfunctional Co-coordination polymers (Pd/CoBDCNH$_2$ and Pd/CoBDC). Advanced analytical techniques revealed that Pd-NPs are supported on the external surface of the polymer framework and the functionalized framework possesses effective influence to prevent Pd-NP aggregation. Supported Pd-NPs were effectively applied as heterogeneous recyclable catalysts in the Mizoroki–Heck C–C cross coupling reactions of iodobenzene and either aromatic or aliphatic terminal alkenes. Catalytic results exhibited that highly dispersed Pd-NPs with low loading (1%) on the functional polymer (Pd/CoBDCNH$_2$) are more effective than aggregated Pd-NPs with high loading (9%) on the nonfunctional polymer (Pd/CoBDC). Both catalysts can simultaneously provide high activity and selectivity to E-coupled products, high efficiency in low amounts, easy separation of heterogeneous catalyst and appropriate performance in the recycling reaction without addition of a reducing agent.

© 2016 Académie des sciences. Published by Elsevier Masson SAS. All rights reserved.

1. Introduction

There has recently been considerable interest in research on the fabrication of metal nanoparticles with high stability and controllable size distribution. This is largely due to their potential application in many fields, especially in catalysis [1–3]. Among catalytically active nanoparticles, palladium nanoparticles (Pd-NPs) have extensively been utilized for the formation of C–C bonds [4–6] that play significant roles in modern synthetic chemistry. The Pd-NPs exhibit suitable catalytic activity. Moreover, heterogeneous metal nanocatalysts provide considerable advantages such as easy isolation of products, efficient recovery and recyclability of catalysts, good

thermal and chemical stabilities, and good dispersion of the active catalytic site [7–9].

A number of solid materials as supports have broadly been investigated for the immobilization of palladium such as clay [10], carbon nanofibers [11], carbon nanotubes [12], graphene [13], ionic liquids [14,15], mesoporous silica [16], zeolites [17], SBA-15 [18], metal oxides [19,20] and polymers [21]. Among these solid supports, metal–organic frameworks (MOFs) or porous coordination polymers can be considered as a suitable solid material for the stabilization of ligand-free metal nanoparticles [22,23]. On the other hand, finding a suitable support to immobilize Pd-NPs without agglomeration is still a tempting challenge in the field of heterogeneous catalysis.

Here, we report the comparative study on the functional effect of polymers on the dispersion and catalytic activity of supported Pd-NPs. We used functional and nonfunctional

* Corresponding author.
E-mail address: f.ashouri@iaups.ac.ir (F. Ashouri).

Co-coordination polymers, Pd/CoBDCNH$_2$ and Pd/CoBDC, respectively, as a support for Pd-NPs where CoBDCNH$_2$ = [Co$_3$(BDCNH$_2$)$_3$(DMF)$_2$(H$_2$O)$_2$]$_n$, CoBDC = [Co$_3$(BDC)$_3$(DMF)$_2$(H$_2$O)$_2$]$_n$, H$_2$BDCNH$_2$ = 2-amino-1,4-benzenedicarboxylic acid and H$_2$BDC = 1,4-benzendicarboxylic acid. Catalytic activity of these supported Pd-NPs was examined in the Mizoroki–Heck coupling reactions of iodobenzene with terminal alkenes.

2. Experimental

2.1. Materials and instruments

All reagents for synthesis and analysis were obtained commercially and of analytical grade and used without further purification. The elemental analysis (CHN) of compound was performed using a Carlo ERBA Model EA 1108 analyzer. Fourier transform infrared (FT-IR) spectroscopy was carried out by utilizing a Unicam Matson 1000 FT-IR spectrophotometer using KBr disks at room temperature. Thermogravimetric analysis (TGA) was performed on a Perkin Elmer TGA7 analyzer in a N$_2$ atmosphere with a heating rate of 5 °C min^{-1}. Powder X-ray diffraction (XRD) patterns were recorded by using a Rigaku D-max C III and X-ray diffractometer using Ni-filtered Cu Kα radiation. Inductively coupled plasma–mass spectroscopy (ICP-MS) was performed by using an ICP-MS HP 4500. The morphology and size of palladium nanoparticles in Pd/MnBDC were investigated by incorporating scanning electron microscopy (SEM, S-4160, Hitachi) and high-resolution transmission electron microscopy (HR-TEM, Philips CM30) at 300 kV. X-ray photoelectron spectroscopy (XPS) measurements were performed on a PerkinElmer PHI 5000CESCA system with a base pressure of 10^{-9} Torr. The products of the coupling reaction were determined and analyzed by using an HP Agilent 6890 gas chromatograph equipped with an HP-5 capillary column (phenyl-methylsiloxane 30 m × 320 μm × 0.25 μm) and a flame-ionization detector.

2.2. Synthesis of the [Co$_3$(BDC)$_3$(DMF)$_2$(H$_2$O)$_2$]$_n$ framework

The [Co$_3$(BDC)$_3$(DMF)$_2$(H$_2$O)$_2$]$_n$ coordination polymer (CoBDC) was synthesized based on our previous study [24] by adding a solution of 1,4-benzenedicarboxylic acid (H$_2$BDC) (166 mg, 1 mmol) in 5 mL of DMF to CoCl$_2$·6H$_2$O (291 mg, 1 mmol) solution (DMF, 5 mL). The solution was heated for 48 h at 80 °C. After 2 days, purple crystals of [Co$_3$(BDC)$_3$(DMF)$_2$(H$_2$O)$_2$]$_n$ (85% yield based on H$_2$BDC) were collected. Anal. Calcd: for Co$_3$C$_{30}$H$_{24}$N$_2$O$_{16}$: C, 42.42; H, 3.32; N, 3.30. Found: C, 42.63; H, 2.86; N, 3.28. FT-IR (KBr 4000–400 cm^{-1}): 3491 (br), 2931 (w), 1663 (s), 1619 (s), 1559 (s), 1418 (s), 1254 (w), 1115 (m), 855 (m), 813 (m), 760 (s), 693 (s), 655 (m), 468 (m).

2.3. Synthesis of the [Co$_3$(BDCNH$_2$)$_3$(DMF)$_2$(H$_2$O)$_2$]$_n$ framework

A DMF solution (5 mL) of CoCl$_2$·6H$_2$O (291 mg, 1 mmol) was added to a solution of 2-amino-1,4-benzene dicarboxylic acid (H$_2$BDCNH$_2$) (182 mg, 1 mmol) in 5 mL of DMF in a small sample vessel. The solution was heated for 24 h at 90 °C. A light cream powder of [Co$_3$(BDC NH$_2$)$_3$(DMF)$_2$(H$_2$O)$_2$]$_n$ (named CoBDCNH$_2$, 85% yield based on H$_2$BDCNH$_2$) was obtained as an amino-functionalized polymer. The crystals were washed with DMF (3 mL, 2 times) and dried at 80 °C. Anal. Calcd: for Co$_3$C$_{30}$H$_{33}$N$_5$O$_{16}$: C, 40.19; H, 3.71; N, 7.81. Found: C, 40.72; H, 3.70; N, 7.75. FT-IR (KBr 4000–400 cm^{-1}): 3491 (br), 2931 (w), 1663 (s), 1619 (s), 1559 (s), 1418 (s), 1254 (w), 1115 (m), 855 (m), 813 (m), 760 (s), 693 (s), 655 (m), 468 (m).

2.4. Synthesis of supported palladium nanoparticles on the CoBDC polymer framework

The prepared CoBDC polymer (0.15 g) was added to an orange solution of PdCl$_2$ (0.04 g, 0.2 mmol) and NaCl (0.58 g, 1.0 mmol) in DMF (10 mL) under vigorous stirring. Upon adding hydrazine hydrate (4 mL, excess), the mixture immediately turned gray. After stirring for 15 min, the solid was isolated by centrifugation, washed with DMF and dried in an oven at 90 °C. Supported Pd nanoparticles on the Co-coordination polymer (Pd/CoBDC) was obtained as a gray powder. The Pd contents (9 wt %) in the samples were determined by ICP-MS. FT-IR (KBr 4000–400 cm^{-1}): 3475 (br), 3332 (br), 2935 (w), 1659 (w), 1560 (s), 1555 (m), 1419 (s), 1358 (m), 1142 (m), 855(m), 828 (w), 807 (w), 732 (s), 695 (s), 529 (w), 480 (w).

2.5. Synthesis of supported palladium nanoparticles on the CoBDCNH$_2$ polymer framework

The supported Pd-NPs on the amino-functionalized Co-coordination polymer (Pd/CoBDCNH$_2$) was obtained as a gray powder by the addition of an orange solution of PdCl$_2$ (0.04 g, 0.2 mmol) and NaCl (0.58 g, 1.0 mmol) in DMF (10 mL) to prepare CoBDCNH$_2$ (0.15 g) in the presence of hydrazine hydrate (4 mL, excess). After stirring for 15 min, the solid was isolated by centrifugation, washed with DMF and dried in an oven at 90 °C. The Pd contents (1 wt %) in the samples were determined by ICP-MS. FT-IR (KBr 4000–400 cm^{-1}): 3485 (br), 2930 (w), 1659 (s), 1620 (s), 1550 (m), 1420(s), 1250 (w), 1102 (m), 850 (m), 810 (m), 765 (s), 690 (s), 650 (m), 460 (m).

2.6. General procedure for Heck coupling reactions catalyzed by Pd/CoBDC and Pd/CoBDCNH$_2$ catalysts

The heterogeneous C–C coupling reaction was conducted in a two-necked round-bottom flask fitted to a condenser and magnetic stirrer and placed in a temperature-controlled oil bath. Typically, 1.1 mmol of the substrate was taken in 2 mL of solvent, followed by the addition of 13 mg Pd/CoBDC (0.11 mol % Pd) or 5 mg Pd/CoBDCNH$_2$ (0.05 mol % Pd) catalyst, 1 mmol iodobenzene and 1.5 mmol base. The flask was kept at 90 °C and stirred at appropriate times. The products from the reaction mixture were analyzed by gas chromatography and were identified by comparison to known standards.
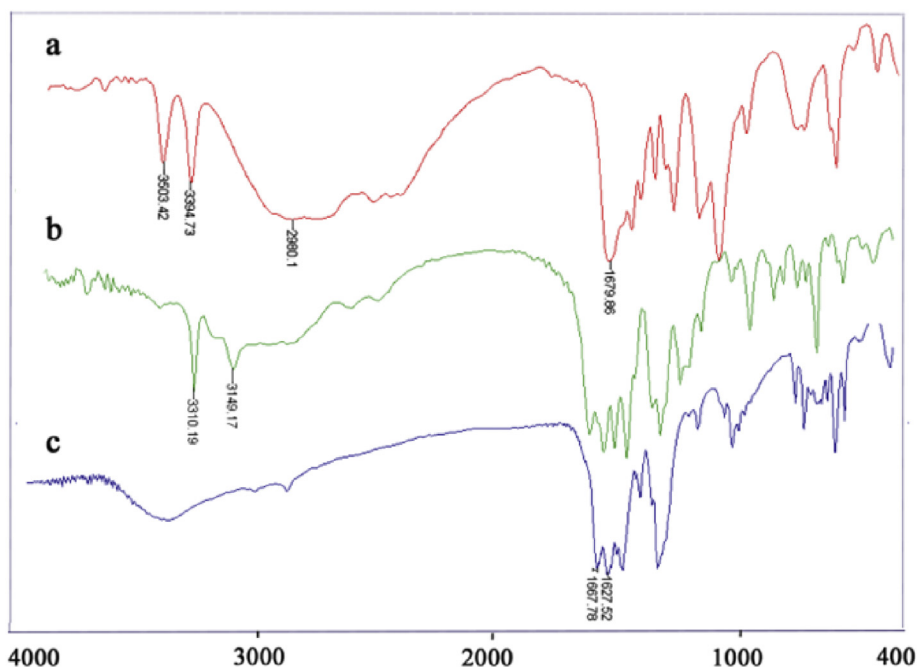
Fig. 1. FT-IR spectrum of the H_2BDCNH_2 ligand (a) and CoBDCNH$_2$ (b) and CoBDC (c) polymers.

3. Results and discussion

3.1. Characterization of the polymer framework and supported Pd nanoparticles

The $[Co_3(BDC)_3(DMF)_2(H_2O)_2]_n$ framework was synthesized and characterized based on our previous reported work [24]. The CoBDC polymer is made of Co−O$_6$ octahedral linked by H_2BDC ligands. The coordination polymer structure is a 2D-periodic framework formed by two-dimensional infinite straightforward chains through covalent interactions.

The CoBDCNH$_2$ framework was synthesized in the same way but the attempt to obtain its suitable single crystal was unsuccessful. Therefore, the amino-functionalized framework of CoBDCNH$_2$ was characterized based on solid powder.

The differences between the functional and nonfunctional polymers are very obvious in the FT-IR spectra of these polymers (Fig. 1). The finger point area for −NH$_2$ functional group is distinguishable in free ligands (Fig. 1a) and the Co-amino-functionalized polymer (Fig. 1b). These peaks appear at 3503 and 3394 cm^{-1} in free ligands and at 3310 and 3149 cm^{-1} in the amino-functionalized polymer, respectively. The existence of these peaks in the polymer indicates that the functional group remained unchanged after polymer formation. The slight shifts are due to the ortho effects of amino and carboxylate groups that happen after framework formation. The absence of these finger point peaks in the Co-nonfunctional polymer is the obvious difference between these two polymers (Fig. 1c).

Fig. 2 demonstrates the following coordination modes in H_2BDCNH_2 linker ligand from carboxylate groups to the metal centers that help to form a polymer framework.
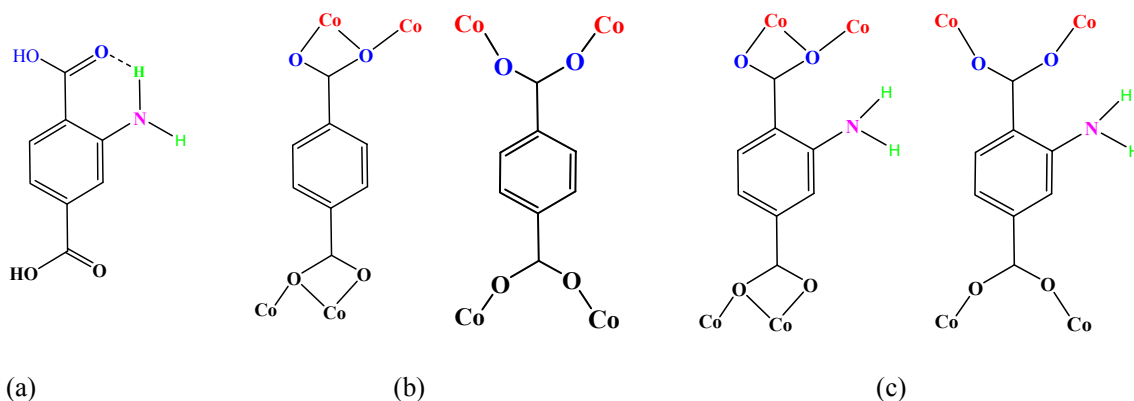

(a) (b) (c)

Fig. 2. The inter-hydrogen bond in the H_2BDCNH_2 linker ligand (a), coordination modes in the nonfunctional polymer (b) [25], and in the amino-functionalized polymer (c).
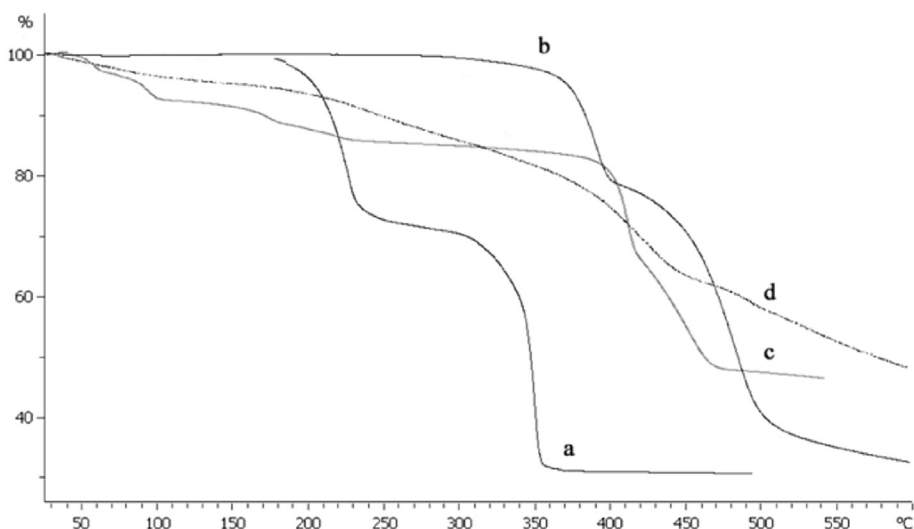
Fig. 3. TGA curves of CoBDC (a), CoBDCNH$_2$ (b), Pd/CoBDC (c) and Pd/CoBDCNH$_2$ (d) coordination polymers.

A thermal study shows that both polymers have similar decomposition profiles (Fig. 3). Final destruction occurred at 330–350 °C for CoBDC and at 460–490 °C for the Co-BDCNH$_2$ polymer. It seems that the functionalized polymer has a higher thermal stability. The first major mass loss step of 19.56% at 380 °C in Co-BDCNH$_2$ polymer was attributed to the removal of 2 DMF and 2 water molecules per formula unit (calcd. 20.04%). Furthermore, upon further heating, there was no mass loss until the structure collapsed at 460–480 °C (weight loss 43.56%). These weight losses are in agreement with $[Co_3(BDCNH_2)_3(DMF)_2(H_2O)_2]_n$ empirical formula. This supposed formula of the Co-BDCNH$_2$ polymer was further confirmed by elemental analysis.

The solution impregnation method was used to immobilize Pd-NPs on the functional and nonfunctional Co-coordination polymers (Pd/CoBDCNH$_2$ and Pd/CoBDC).

The TGA analysis of supported PdNPs on the CoBDC polymer (Fig. 3c) exhibited the same destruction profile as CoBDC but with a slow loss of weight. The weight loss started at 80 °C and continued to 160 °C, then reached 400 °C by a constant slope. Final collapse occurred at 420–470 °C. The weight loss in Pd/CoBDCNH$_2$ polymer started at 100–300 °C by gentle slope and continued to 340–450 °C by steep slope. The final decomposition of this polymer occurred at 530 °C–600 °C. It seems that the presence of active Pd-NPs on polymers is due to the simple degradation of organic moieties [25].

As shown in the XRD pattern, the presence of PdNPs had no influence on the structural characteristics of the polymers and there is no significant loss of crystallinity in framework diffraction patterns after PdNP loading (Fig. 4). The characteristic peaks of Pd (111) and Pd (200) at $2\theta = 40.10$ and 46.5°, respectively, are distinguishable.

The size and local composition of PdNPs were investigated by HR-TEM (Fig. 5). The images obviously show that the highly aggregated Pd-NPs are attached to the polymer surface (Fig. 5a,b). EDX spectroscopy confirmed the presence of aggregated Pd-NPs on the external surface of the

CoBDC coordination polymer. As observed in Pd/MIL-53(Al) [4], this aggregation was predictable due to the nonfunctionalized polymer framework [4,23]. PdNPs were well dispersed on the surface of CoBDCNH$_2$ polymers (Fig. 5c and d). It seems that the functionalized polymer possesses an effective influence to prevent the aggregation of particles. Another difference between functionalized and nonfunctionalized polymers is the morphology. It was observed from the SEM images that the change in morphology occurs from nanospheres in the CoBDC polymer to nanosheets in the CoBDCNH$_2$ polymer due to functionalized linker ligands (Fig. 6). It is obvious that the morphology remains unchanged after the loading of PdNPs.
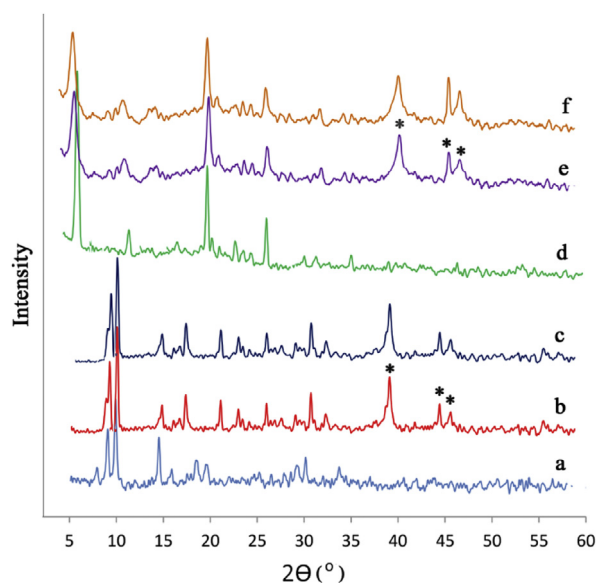

Fig. 4. Powder XRD patterns of CoBDC (a), Pd/CoBDC before (b) and after four circles in the catalysis reaction (c), CoBDCNH$_2$ (d) and Pd/CoBDCNH$_2$ before (e) and after four cycles in the catalysis reaction (f). The 2θ values characteristic for palladium are highlighted (*).
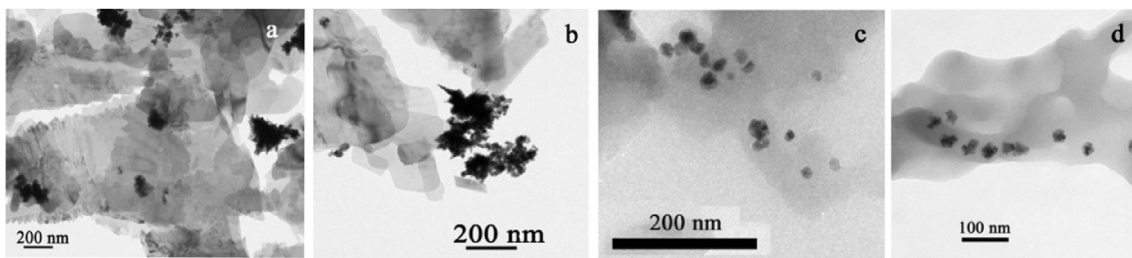
Fig. 5. TEM images of supported Pd-NPs on CoBDC (a, b) and CoBDCNH$_2$ (c, d) polymer framework.
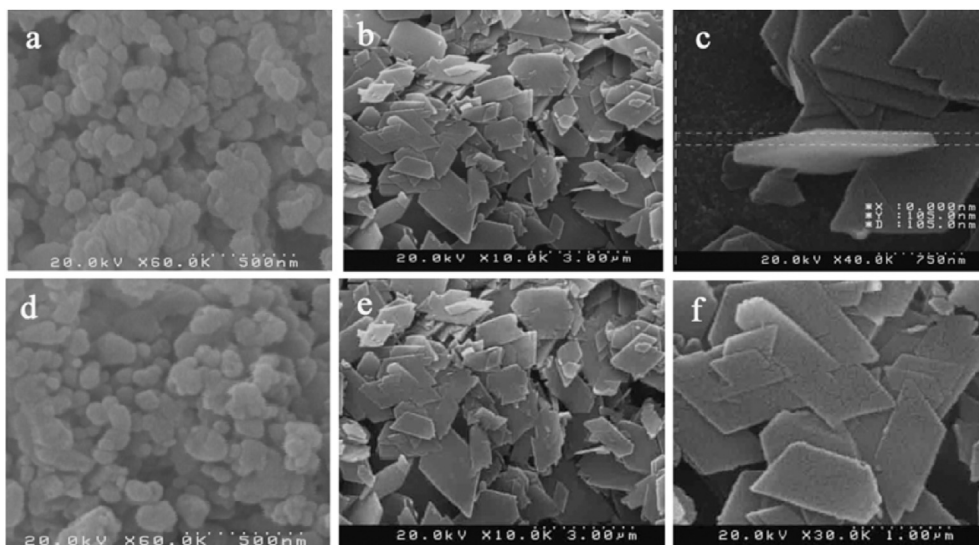

Fig. 6. SEM images of CoBDC (a), CoBDCNH$_2$ (b, c), Pd/CoBDC (d) and Pd/CoBDCNH$_2$ (e, f).

Using the Debye−Scherer equation, the average diameter of Pd-NPs was estimated to be 30 nm for Pd/CoBDC and 40 nm for Pd/CoBDCNH$_2$, which matched very well with TEM data as estimated by size distribution. The Pd contents in Pd/CoBDC and Pd/CoBDCNH$_2$ polymers were determined (9% and 1% wt, respectively) by inductively coupled plasma−mass spectroscopy (ICP-MS).

The X-ray photoelectron spectroscopy measurement (XPS) study demonstrated that the Pd species in polymers are present in the metallic state (Fig. 7). This is verified by the two peaks with a binding energies of 335.6 and 341.1 eV in Pd/CoBDC (Fig. 7a) and 336.3 and 341.9 eV in Pd/CoBDCNH$_2$ (Fig. 7b) in the 3d$_{5/2}$ and 3d$_{3/2}$ levels of Pd(0), respectively. Photoelectrons emitted from carboxyl groups,
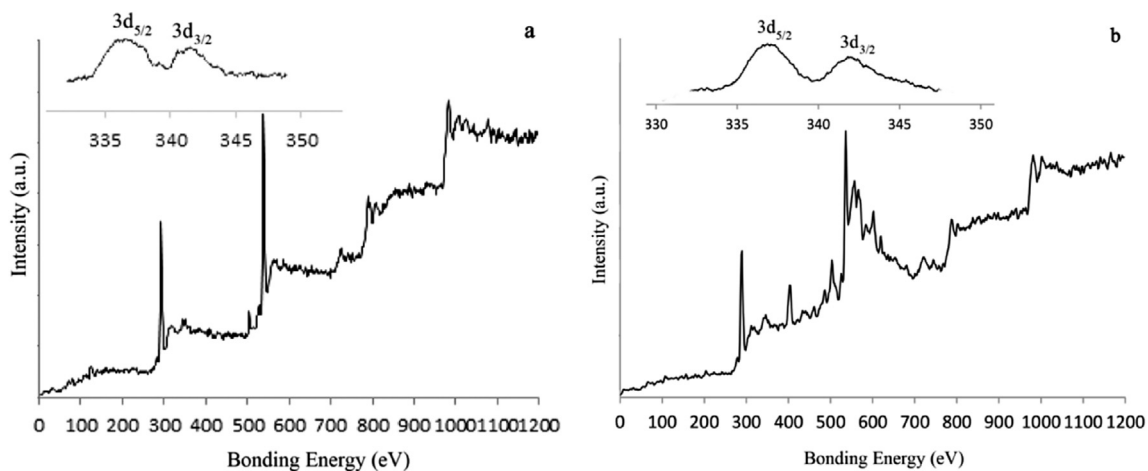

Fig. 7. Wide scan XPS spectra of the Pd/CoBDC (a) and Pd/CoBDCNH$_2$ (b) with Pd core level spectra.

C 1s and O 1s core level in the 1,4-benzenedicarboxylate linker in Pd/CoBDC, generated peaks centered at 284 and 533 eV binding energy, respectively [23]. Photoelectrons emitted from carboxyl groups and an amine branch, C 1s, N 1s and O 1s core level in Pd/CoBDCNH$_2$, generated peaks centered at 285.5, 399.8 and 532 eV binding energy, respectively. The peaks at 788 and 800 eV were assigned to Co(2p$_{3/2}$) and Co(2p$_{1/2}$) in the Co-O$_6$ environment, respectively [26].

3.2. Mizoroki–Heck coupling reaction of iodobenzene and terminal alkenes in the presence of supported Pd-NPs

The coupling of C–C bonds constitutes significant reactions in organic chemistry that can lead to a diverse range of derivatives. Therefore, the catalytic activity of supported PdNPs on the coordination polymers was applied to the Mizoroki–Heck coupling reaction. In order to find the suitable reaction conditions to achieve the maximum yield of the Mizoroki–Heck reaction, conditions such as solvent, base and reaction temperature were studied by choosing styrene and iodobenzene as a model reaction (Table 1). The excellent yields of products were obtained in dimethylacetamide (DMA) (entries 1–5) even at a lower temperature (entry 14). Among the different organic and inorganic bases, the highest conversion of coupling reactions was observed in the presence of Et$_3$N base (entries 3, 8, 11–13). A controlled experiment indicated that no cross-coupling product was observed in the absence of the catalyst or base (entries 15, 16).

The coupling between iodobenzene and various terminal alkenes has been investigated under the above-optimized reaction conditions, Et$_3$N as the base and DMA as the solvent at 90 °C (Table 2). The results show that in the presence of supported PdNPs, alkenes with either electron-withdrawing or electron-donating substituents react with

Table 1
Optimization of the reaction conditions in the cross coupling reaction of iodobenzene and styrene in the presence of Pd/CoBDC and Pd/CoBDCNH$_2$ catalysts.[a]
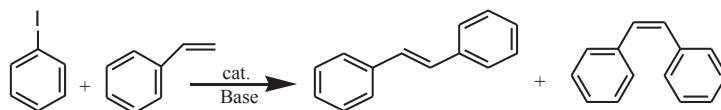
Entry	Catalyst	Solvent	Base	% Conversion[b]	% Selectivity[c]
1	Pd/CoBDC	DMSO	Et$_3$N	80	90
	Pd/CoBDCNH$_2$			80	95
2	Pd/CoBDC	DMF	Et$_3$N	87	88
	Pd/CoBDCNH$_2$			90	90
3	Pd/CoBDC	DMA	Et$_3$N	95	92
	Pd/CoBDCNH$_2$			97	95
4	Pd/CoBDC	CH$_3$CN	Et$_3$N	55[d]	85
	Pd/CoBDCNH$_2$			50[d]	85
5	Pd/CoBDC	p-xylene	Et$_3$N	20	70
	Pd/CoBDCNH$_2$			25	75
6	Pd/CoBDC	DMSO	K$_2$CO$_3$	60	85
	Pd/CoBDCNH$_2$			55	85
7	Pd/CoBDC	DMF	K$_2$CO$_3$	70	85
	Pd/CoBDCNH$_2$			75	85
8	Pd/CoBDC	DMA	K$_2$CO$_3$	75	82
	Pd/CoBDCNH$_2$			78	82
9	Pd/CoBDC	DMSO	NaCH$_3$CO$_2$	70	82
	Pd/CoBDCNH$_2$			70	82
10	Pd/CoBDC	DMF	NaCH$_3$CO$_2$	82	90
	Pd/CoBDCNH$_2$			82	90
11	Pd/CoBDC	DMA	NaCH$_3$CO$_2$	85	90
	Pd/CoBDCNH$_2$			85	90
12	Pd/CoBDC	DMA	Pyridine	15	85
	Pd/CoBDCNH$_2$			17	87
13	Pd/CoBDC	DMA	Pyrrolidine	13	87
	Pd/CoBDCNH$_2$			10	85
14	Pd/CoBDC	DMA	Et$_3$N	70[e]	88
	Pd/CoBDCNH$_2$			65[e]	85
15	Pd/CoBDC	DMA	–	1	–
	Pd/CoBDCNH$_2$			2	–
16	–	DMA	Et$_3$N	1[f]	–
	–			1[f]	–

[a] Reaction conditions: 13 mg Pd/CoBDC (0.11 mol % Pd), 5 mg Pd/CoBDCNH$_2$ (0.05 mol % Pd), styrene 1.1 mmol, iodobenzene 1 mmol, base 1.5 mmol, temperature 90 °C, after 9 h.
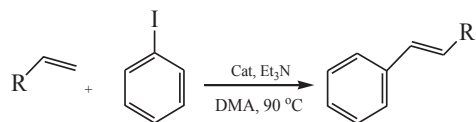[b] Determined by GC, based on iodobenzene; average of two runs.
[c] Selectivity to trans-stilbene.
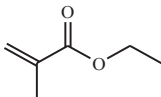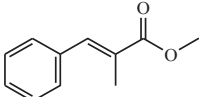[d] Solvent boiling point.
[e] Temperature 70 °C.
[f] Reaction without catalyst.

Table 2
The coupling reaction of iodobenzene and terminal alkenes catalyzed by Pd/CoBDC and Pd/CoBDCNH$_2$.[a]

Entry	Catalyst	Olefin	% Conversion[b]	% Selectivity to product
1	Pd/CoBDC Pd/CoBDCNH$_2$		95 97	92 95
2	Pd/CoBDC Pd/CoBDCNH$_2$		85 85	90 90
3	Pd/CoBDC Pd/CoBDCNH$_2$		84 75	88 90
4	Pd/CoBDCNH$_2$ Pd/CoBDC		15 15	90 90
5	Pd/CoBDC Pd/CoBDCNH$_2$		90 90	85 86
6	Pd/CoBDC Pd/CoBDCNH$_2$		95 99	100 100
7	Pd/CoBDC Pd/CoBDCNH$_2$		85 98	100 100
8	Pd/CoBDC Pd/CoBDCNH$_2$		80 80	77 78
9	Pd/CoBDC Pd/CoBDCNH$_2$		55 55	60 65

(*continued on next page*)

Table 2 (*continued*)

Entry	Catalyst	Olefin	% Conversion[b]	% Selectivity to product
10	Pd/CoBDC Pd/CoBDCNH$_2$		75 80	92 90

^a Reaction conditions: 13 mg Pd/CoBDC (0.11 mol % Pd), 5 mg Pd/CoBDCNH$_2$ (0.05 mol % Pd), 1.1 mmol substrate, 1 mmol iodobenzene, 1.5 mmol Et$_3$N, in DMA solvent, temperature 90 °C, after 9 h.
^b Determined by GC, based on iodobenzene; average of two runs.

iodobenzene, rapidly forming the corresponding coupled products with good yields and excellent selectivity to E-isomeric products (Table 2). The conversion and selectivity of products show that the coupling reactions catalyzed by both catalysts proceed through the same mechanism proposed in the literature [23].

The recyclability of the supported Pd-NPs catalyst was investigated in the reaction of styrene with iodobenzene using Et$_3$N/DMA at 90 °C for 9 h in the presence of Pd/CoBDC (13 mg, 0.11 mol % Pd) and Pd/CoBDCNH$_2$ (5 mg, 0.05 mol % Pd). The solid catalyst was easily isolated by centrifugation after the first catalytic reaction and recovered by being washed with the solvent and dried at 80 °C. Afterwards, it was used for the next run under the same reaction conditions. The catalytic activity was found to remain almost unchanged even after four cycles, without significant degradation in activity and selectivity to *trans*-stilbene as a major E-product (Table 3).

The catalytic results show that supported PdNPs on polymers are active catalysts in the C–C coupling reaction. For C-C coupling reaction of iodobenzene and terminal olefins, amount of 13 mg (0.11 mol % Pd) from Pd/CoBDC catalyst and 5 mg (0.05 mol % Pd) from Pd/CoBDCNH2 catalyst, were used. So, from a catalytic point of view, the Pd/CoBDCNH$_2$ is superior in terms of the amount of the catalyst. It seems that highly dispersed and low loading PdNPs on CoBDCNH$_2$ (1%) are efficient than aggregated and high loading Pd-NPs on CoBDC (9%). This fact demonstrates the functionality effect of the polymer on catalyst efficiency.

Table 3
The reusability and palladium leaching test in the Mizoroki–Heck coupling reaction of iodobenzene with styrene catalyzed by Pd/CoBDC and Pd/CoBDCNH$_2$ heterogeneous catalysts.^a

Entry	Catalyst	Conversion (%)	Selectivity (%)[b]	% Pd[c]
Run 1	Pd/CoBDC	95	92	0.15
	Pd/CoBDCNH$_2$	97	95	0.02
Run 2	Pd/CoBDC	91	92	0.08
	Pd/CoBDCNH$_2$	95	95	0.007
Run 3	Pd/CoBDC	87	91	0.05
	Pd/CoBDCNH$_2$	92	95	0.004
Run 4	Pd/CoBDC	85	91	0.02
	Pd/CoBDCNH$_2$	88	94	<0.001

^a Reaction conditions: same as those in Table 2.
^b Selectivity (%) to E-product.
^c The palladium content in the solution, determined by ICP-MS.

Since some of the active sites in the solid catalyst could dissolve into the solution during the catalytic reaction, the amount of palladium in solution after each catalytic run was determined by ICP-MS to find whether palladium leaching occurs during the reaction. Therefore, after the first catalytic reaction of iodobenzene and styrene by Pd/CoBDC and Pd/CoBDCNH$_2$, the heterogeneous catalyst was simply separated from the reaction mixture by centrifugation and the content of palladium in solution was determined by ICP-MS (Table 3). The leaching test after each catalytic run revealed that the amount of palladium leached from the catalyst to solution is very negligible. Moreover, fresh reagents were added to the solution and stirred at 90 °C. Only less than 6% conversion was observed after 24 h for both catalysts. Therefore, there is no contribution of catalytically active palladium leached species in solution.

In order to further confirm that the reaction was indeed catalyzed by supported PdNPs instead of free Pd-NPs in styrene and iodobenzene coupling reaction, a hot filtration test was carried out by stopping the reaction after 3 h. The reaction reached 25 and 32% conversion for Pd/CoBDC and Pd/CoBDCNH$_2$, respectively. Then the catalyst was separated from the reaction mixture and reaction was continued. The conversion was increased by 6 and 7%, respectively, after 24 h. These results confirmed that the coupling reaction could only continue in the presence of the solid catalyst, and there was no contribution from the homogeneous catalysis of leached active species in the liquid phase.

The XRD patterns of catalysts after the reaction displayed the same diffraction profile and relatively similar intensity that indicated that the catalysts retained a well-crystallized structure after the catalytic reaction (Fig. 4c,f).

4. Conclusion

Supported palladium nanoparticles (Pd-NPs) on the functional and nonfunctional Co-coordination polymers were prepared using a solution impregnation method. Pd-NPs are highly dispersed on the functional polymer with an average diameter of 30 nm and a loading of 1%, while the nonfunctional polymer showed high loading (9%) and aggregated Pd-NPs with an average diameter of 40 nm. Therefore, not only does the functional framework prohibit the aggregation of Pd-NPs, but it also causes the catalyst Pd/CoBDCNH$_2$ to show high efficacy in comparison to Pd/CoBDC despite being less in amount (5 mg Pd/CoBDCNH$_2$,

0.05 mol % Pd and 13 mg Pd/CoBDC, 0.11 mol % Pd). This exhibits the prominence of the framework function. Supported Pd-NPs were proved to be highly active and stable catalysts for the C—C coupling reaction of aromatic and aliphatic terminal alkenes in excellent yields and selectivity to E-products in the Mizoroki—Heck reactions. The noticeable advantages of these heterogeneous catalytic systems are low leaching, high efficiency in low amounts, selectivity to E-products, easy separation of catalysts and appropriate performance in the recycling reaction.

Acknowledgements

References

[1] M. Amini, M.M. Najafpourb, M. Zared, E. Amini, J. Mol. Catal. A Chem. 394 (2014) 303.
[2] M. Amini, H. Naslhajian, S. Morteza, F. Farnia, New J. Chem. 38 (2014) 1581.
[3] M. Zahmakiran, S. Özkar, Nanoscale 3 (2011) 3462.
[4] V. Chandrasekha, R.S. Narayanan, Tetrahedron Lett. 52 (2011) 3527.
[5] X. Nie, S. Liu, Y. Zong, P. Sun, J. Bao, J. Organomet. Chem. 696 (2011) 1570.
[6] Y. Huang, Z. Zheng, T. Liu, J. Lü, Z. Lin, H. Li, R. Cao, Catal. Commun. 14 (2011) 27.
[7] F. Coccia, L. Tonucci, N. Alessandroc, P. D'Ambrosioc, M. Bressanc, Inorg. Chim. Acta 399 (2013) 12.
[8] E. Ramirez, S. Jansat, K. Philippot, P. Lecante, M. Gomez, A.M. Masdeu-Bulto, B. Chaudret, J. Organomet. Chem. 689 (2004) 4601.
[9] D.E. De Vos, M. Dams, B.F. Sels, P.A. Jacobs, Chem. Rev. 102 (2002) 3615.
[10] K.K.R. Datta, M. Eswaramoorthy, C.N.R. Rao, J. Mater. Chem. 17 (2007) 613.
[11] J. Zhu, J. Zhou, T. Zhao, X. Zhou, D. Chen, W. Yuan, Appli. Catal. A General 352 (2009) 243.
[12] F. Yanga, C. Chi, S. Donga, C. Wangb, X. Jiaa, L. Rena, Y. Zhanga, L. Zhanga, Y. Li, Catal. Today 02 (2015) 026. DOI: 10.1016/j. cattod. 2015.
[13] S.S. Shendage, U.B. Patil, J.M. Nagarkar, Tetrahedron Lett. 54 (2013) 3457.
[14] P. Cotugno, M. Casiello, A. Nacci, P. Mastrorilli, M.M. Dell'Anna, A. Monopoli, J. Organomet. Chem. 752 (2014) 1.
[15] J. Li, X.Y. Shi, Y.Y. Bi, J.F. Wei, Z.G. Chen, ACS Catal. 1 (2011) 657.
[16] S.M. Quarrie, B. Nohair, J.H. Horton, S. Kaliaguine, C.M. Crudden, J. Phys. Chem. C 114 (2010) 57.
[17] M. Choi, D.H. Lee, K. Na, B.W. Yu, R. Ryoo, Angew. Chem. Int. 48 (2009) 3673.
[18] Z. Zheng, H. Li, T. Liu, R. Cao, J. Catal. 270 (2010) 268.
[19] L. Zhang, Z. Meng, S. Zang, J. Environ. Sci. 31 (2015) 194.
[20] A.J. Amali, R.K. Rana, Green Chem. 11 (2009) 1781.
[21] M.M. Dell'Annaa, M. Malia, P. Mastrorilli, A. Rizzutia, C. Ponzonic, C. Leonellic, J. Mol, Catal. A Chem. 366 (2013) 186.
[22] M. Gulcana, M. Zahmakirana, S. Özkar, Appl. Catal. B Environ. 147 (2014) 394.
[23] M. Bagherzadeh, F. Ashouri, L. Hashemi, A. Morsali, Inorg. Chem. Commun. 44 (2014) 10.
[24] M. Bagherzadeh, F. Ashouri, M. Đaković, J. solid State Chem. 223 (2015) 32.
[25] S. Gao, N. Zhao, M. Shu, S. Che, Appli. Catal. A General 388 (2010) 196.
[26] K. Burger, H. Ebel, M. Ebel, C.S. Varhelyi, Inorg. Chim. Acta 88 (1984). Lll.